

A Nickel–Carbon Eutectic Cell for Contact and Non-contact Thermometry

Renato Nunes Teixeira · Antônio Carlos Baratto

Published online: 23 October 2007
© Springer Science+Business Media, LLC 2007

Abstract The highest-temperature, defining fixed point of the International Temperature Scale of 1990 (ITS-90) is the copper freezing point (1,084.62°C). Many international metrology institutes are investigating the use of transition temperatures of metal–carbon alloys as references for the calibration of temperature measuring instruments above the copper point, making it possible to reduce the calibration uncertainty of pyrometers in radiation thermometry and thermocouples in contact thermometry. This research is being performed mainly by radiation thermometry laboratories that have developed specific cells with blackbody cavities containing relatively small quantities of metal–carbon alloys. Parallel to this, some laboratories have also developed cells with these same alloys, but of a different design, suitable for the calibration of thermocouples. This report concerns the development of a nickel–carbon eutectic cell ($\cong 1,329^\circ\text{C}$) at Inmetro, with which either a radiation thermometer or thermocouple can be calibrated. The measurements of the temperature of this cell were performed using the reference radiation thermometer of the Pyrometry Laboratory and Pt/Pd thermocouples that were constructed, stabilized, and calibrated at the Thermometry Laboratory. Details of the cell fabrication, as well as the instrumentation used for the measurements are given. The results of a comparison between the two different types of measurement are reported, including the uncertainty budgets of both methods.

Keywords Eutectics · High temperatures · Nickel · Pyrometry · Thermocouples

R. N. Teixeira (✉) · A. C. Baratto
Divisão de Metrologia Térmica, Instituto Nacional de Metrologia, Normalização e Qualidade Industrial-Inmetro, Av. N. Sra. das Graças, 50, Xerém, Duque de Caxias, Rio de Janeiro 25250-020, Brazil
e-mail: rnteixeira@inmetro.gov.br

1 Introduction

The calibration of temperature measuring sensors above the freezing point of copper is performed in different ways, most of them having relatively large uncertainties, e.g., like the wire bridge method for thermocouples at the Pd melting point. The International Temperature Scale of 1990 (ITS-90) [1] does not elaborate methodologies for performing these calibrations with the uncertainties that are increasingly required by upcoming high technology applications. In 1996, a joint committee of the Consultative Committee for Photometry and Radiometry (CCPR) and the Consultative Committee for Thermometry (CCT) recommended the development of high-temperature fixed-point blackbody sources above the copper freezing point [2]. Currently, the most promising candidates, not only for radiation thermometry but also for contact thermometry, are the metal carbon eutectic fixed points first realized by Yamada et al. at NMIJ [3]. During the last 8 years, much research has been undertaken to qualify metal–carbon eutectic fixed points so they can be used to reduce the uncertainties in the calibration of high-temperature thermometers. A good review of the current state of high-temperature fixed-point research is found in [4]. Many of the measurements in this temperature range are performed using radiation thermometers; this explains why high-temperature fixed points exceeding 2,800°C have been investigated. High-temperature fixed points up to 2,000°C could potentially be used to calibrate W-Re thermocouples. For lower temperatures (<1,500°C), suitable high-temperature fixed points have been identified to calibrate high performance Pt/Pd thermocouples, as well as improve the calibration of noble-metal thermocouples like types R, S, and B. In many metrology institutes, eutectic cells are being developed for use with contact and non-contact thermometry.

At Inmetro, we decided to construct eutectic cells of Ni–C and Fe–C for the calibration of thermocouples, using a vertical furnace. In addition to this development, we decided to construct a eutectic cell that could be used for both contact and radiation thermometry in the horizontal position, though not simultaneously. The material chosen for this dual-use cell was nickel–carbon eutectic, which has an interesting intermediate melting temperature of interest to both contact and non-contact thermometry; the costs involved are not too high, and Ni–C does not present the same operational difficulties as found with Fe–C.

2 Nickel–Carbon Eutectic Fixed-point Cell

The Ni–C cell used in this work was designed and constructed at Inmetro specifically to be used in the horizontal furnace described in Sect. 3. It was constructed from a graphite of high purity (10 ppm nominal) and density (manufactured and machined by Carbone Lorraine). Before the filling of the cell, the graphite parts were baked in an argon atmosphere above the eutectic melting point to remove contaminants [5]. The cell has an external diameter of 32 mm, contains a thermometric well of 8 mm internal diameter, and provides an immersion depth of 95 mm for thermocouples. At the bottom of the thermometric well, there is a cone with an apex angle of 120°. A detailed diagram of the cell is given in Fig. 1. These dimensions yield an estimated

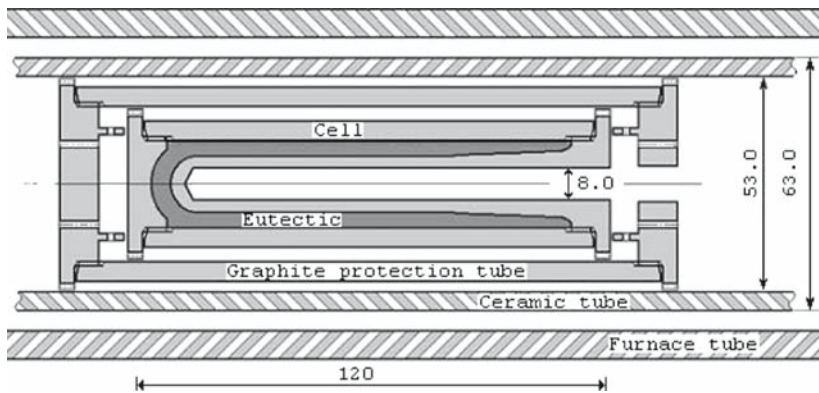


Fig. 1 Ni–C cell assembly inside the furnace tube (dimensions in mm)

emissivity of the blackbody cavity of 0.9999 ± 0.00004 , also taking into account the unlikely possibility of a linear temperature profile of 1°C between the aperture and the conical end of the cavity. This emissivity value was calculated using the model proposed by Bedford and Ma [apud 6]. The nickel and carbon powders were supplied by Alfa Aesar, with a purity of 99.996% for Ni and 99.9999% for C. The powders were mixed at the eutectic composition (1.9% C by mass), and the crucible was filled after five cycles, using a vertical furnace operated in an inert atmosphere with its temperature set to $1,345^\circ\text{C}$ for 45 min to guarantee the complete melting of the charge. The total amount of metal used was 149 g.

The cell was placed inside a second graphite shell in order to offer the graphite crucible extra protection against oxidation and to enhance mechanical strength. The whole assembly was placed inside an alumina tube with an internal diameter of 52 mm. This was subsequently inserted in a tube furnace with an internal diameter of 75 mm.

2.1 Experimental Setup

2.1.1 Furnace

The furnace used was a Carbolite Model TZF 18/75/600 with 10 Kanthal Super heaters divided into three independent zones, controlled by dedicated controllers. The temperature stability of this furnace is typically $0.1^\circ\text{C} \cdot \text{h}^{-1}$ with a temperature uniformity of the order of $\pm 1^\circ\text{C}$ at $1,330^\circ\text{C}$ in the central 15 cm where the cell is located. When hot, there is a continuous flow of 99.999% pure argon through the 75 mm furnace tube to prevent oxidation of the graphite parts.

2.1.2 Radiation Thermometry Measurements

The first measurements of the Ni–C cell constructed at Inmetro were performed by radiation thermometry. For this technique, the temperature was measured using a linear pyrometer from KE, Model LP3, with an interference filter of 650 nm center

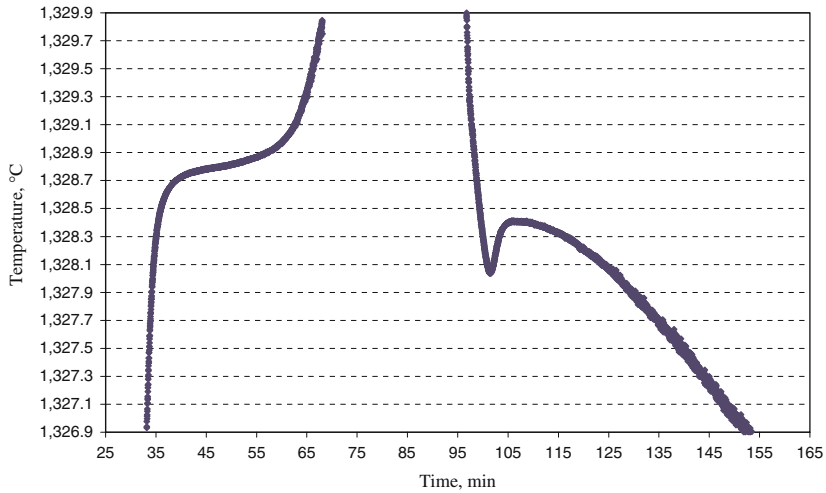


Fig. 2 Melting and freezing plateaux of Ni–C eutectic observed by LP3

wavelength and a bandwidth of 10 nm. This was calibrated at the silver point and checked at the copper point at Inmetro. The target size is approximately 1.1 mm at a measuring distance of 760 mm. Prior to these measurements, the pyrometer had its spectral responsivity evaluated by the Optical Metrology Division of Inmetro [7]. The Ni–C eutectic melting point was determined from the data measured by the LP3 using the inflection point of a third-degree polynomial fitted to the melting plateau. The temperatures determined by the LP3 were calculated using the procedure described by Tischler [8], which takes into account the spectral response of the interference filter and detector. No correction was made for the size-of-source effect. Typical freezing and melting curves are shown in Fig. 2.

2.1.3 Contact Thermometry Measurements

The measurements performed for contact thermometry were made using two Pt/Pd thermocouples that were constructed, stabilized, and calibrated at Inmetro at the freezing points of Sn, Zn, Al, Ag, and Cu. These thermocouples, according to the calibrations performed at Inmetro and at PTB, very closely follow the reference function. Details of the construction of these sensors can be found in [9]. The electromotive forces of the thermocouples were measured using either a Hewlett-Packard Model 3457A 7-1/2 digit multimeter or a Keithley Model 182 nanovoltmeter. The thermocouple reference junctions were kept in ice points. The determination of the Ni–C eutectic melting temperature was made using the inflection point of a third-degree polynomial fitted to the melting plateau in conjunction with a deviation function derived from the calibration of the thermocouples and extrapolated above the Cu point. The freezing-point determination corresponded to the highest value of the plateau after the recovery from the supercooled state. The melting and freezing curves can be seen in Fig. 3.

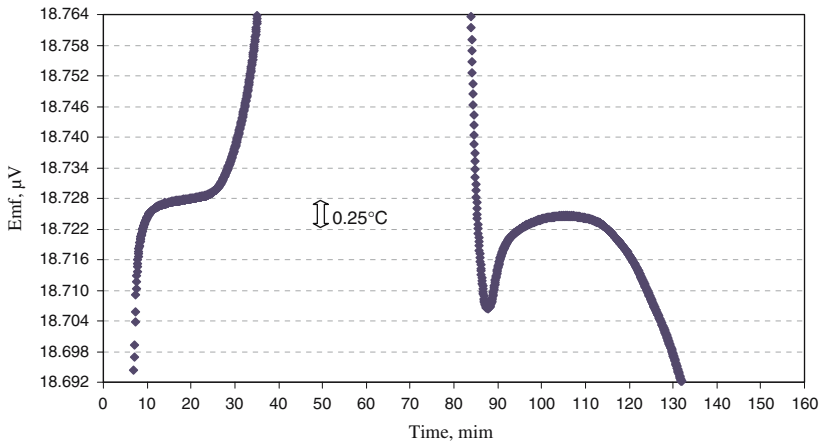


Fig. 3 Melting and freezing plateaux for Ni–C eutectic monitored by Pt/Pd thermocouple

3 Results and Discussion

3.1 Radiation Thermometry

Nine realizations of the Ni–C eutectic cell were performed using the LP3. Due to the relatively large mass of the cell and furnace limitations concerning the heating and cooling rates, it was not possible to have a greater number of realizations in the time available for the measurements. A mean value for the melting point of $1,328.77^{\circ}\text{C}$ with a standard deviation of 0.022°C and a mean value for the freezing point of $1,328.61^{\circ}\text{C}$ with a standard deviation of 0.032°C were achieved. All the measured values for both melts and freezes fall within a temperature interval of 0.25°C . A summary of all the results is shown in Table 1. These results are in agreement with those reported by other researchers [10]. During some runs, it was not possible to observe the supercooled liquid, making the freezing temperature less reliable than the melting temperature. The furnace heating rates varied from 1.5 to $4.8^{\circ}\text{C} \cdot \text{min}^{-1}$. These different heating rates had no effect on the temperature of the melting point. For the freezing point, the furnace cooling rates varied from 2.0 to $4.8^{\circ}\text{C} \cdot \text{min}^{-1}$, impacting the duration of the plateau and also the existence of the supercooled liquid. Typically, the end-point temperatures for the melt and the freeze were set 7 – 8°C higher or lower than the realization temperature, respectively.

The uncertainty budget of the measured eutectic-point temperature by radiation thermometry is shown in Table 2. The uncertainty of the reference cell is the largest contributor to the total uncertainty. The expanded standard uncertainty of the temperature of the Ni–C eutectic cell was 0.26°C , and the estimation of the uncertainty budget followed the procedure described in [11]. Minor contributions were not considered in the evaluation, and conservative estimates were taken for the main sources of uncertainty. The uncertainty of the radiation thermometer, calibrated according to the ITS-90, includes the uncertainties of the silver-point calibration, the spectral responsivity measurement, and the output signal of the radiation thermometer. The

Table 1 Summary of measurements of the melting and freezing temperatures of the Ni–C eutectic cell, measured by the radiation pyrometer

Number of run	Melting temperature (°C)	Freezing temperature (°C)
1	1328.83	1328.55
2	1328.88	1328.49
3	1328.75	N/A ^a
4	1328.84	N/A
5	1328.72	N/A
6	1328.77	1328.70
7	1328.68	1328.60
8	1328.73	1328.66
9	1328.72	1328.65
Mean	1328.77	1328.61
Std.dev.	0.022	0.032

^a Not available, not possible to observe supercooling

Table 2 Uncertainty evaluation of the melting temperature of Ni–C determined by the radiation pyrometer

Quantity X_i	Estimate x_i	Standard uncertainty $u(x_i)$	Probability distribution	Sensitivity coefficient c_i	Uncertainty contribution $u_i(y)$ (°C)
$T(\text{melt})_{\text{Ni-C}}$	1328.77°C	0.022°C	Normal	1	0.022
ε_{BB}	0.9999	0.0001	Normal	$\lambda T^2/C_2$	0.012
T_{Ag}	1234.93 K	0.065 K	Normal	$(T/T_{\text{Ag}})^2$	0.110
Wavelength	650 nm	0.05 nm	Rectangular	$(T/\lambda)(T/T_{\text{Ag}} - 1)$	0.021
Drift	0 nm	0.06 nm	Rectangular	$(T/\lambda)(T/T_{\text{Ag}} - 1)$	0.026
Non-linearity	1	0.0001	Normal	$\lambda/C_2 \cdot T^2 \cdot u(S(T_{\text{Ag}})_L)/S(T_{\text{Ag}})$	0.069
Combined uncertainty					0.135
Expanded uncertainty $k=2$					0.27

$T(\text{melt})_{\text{Ni-C}}$ = melting temperature of the Ni–C cell; ε_{BB} = emissivity of the blackbody cavity of the Ni–C cell; T_{Ag} = temperature of the reference cell (silver) = 1234.93 K; $C_2 = 0.014388 \text{ m} \cdot \text{K}$; $T = 1,602 \text{ K}$; $\lambda = 650 \text{ nm}$; Drift = drift of the spectral response characteristics of the radiation thermometer; $u(S(T_{\text{Ag}})_L)$ = uncertainty from the non-linearity correction; $S(T_{\text{Ag}})$ = signal measured at Ag fixed point

uncertainty of the eutectic-point realization includes the repeatability and the emissivity of the blackbody cavity. For the Ni–C eutectic, the freezing point depends on the cooling rate, which explains the larger standard deviation compared to that of the melting point.

3.2 Contact Thermometry

Twelve realizations of the Ni–C cell were measured using Pt/Pd thermocouples, seven with thermocouple INM2003-03 and five with INM2005-02. A summary of the measurements is given in Table 3. The furnace heating and cooling rates in this case

Table 3 Melting temperatures of the Ni–C cell using Pt/Pd thermocouples

Number of run	Thermocouple/calibration date			
	INM03/03 Feb 2006		INM02/05 Nov 2006	
	Measured emf (μV)	Melting temperature ($^{\circ}\text{C}$)	Measured emf (μV)	Melting temperature ($^{\circ}\text{C}$)
1	18718.86	1328.23		
2	18718.34	1328.20		
3	18719.94	1328.27		
4	18719.16	1328.24		
5	18718.90	1328.23		
6	18717.37	1328.16		
7	18717.54	1328.17		
8			18728.92	1328.38
9			18726.50	1328.28
10			18729.13	1328.39
11			18726.76	1328.29
12			18726.99	1328.30
Mean value		1328.21		1328.33
Std. Dev.		0.015		0.024

varied from 5.0 to $6.0\text{ }^{\circ}\text{C}\cdot\text{min}^{-1}$. For the melt, this change impacted the duration of the plateau, as reported for the radiation thermometry measurements. For the measurements performed with thermocouples, the end-point temperatures for the melting and freezing points were set 5 – 14°C higher or lower than the eutectic temperature, respectively. The melting temperature of the Ni–C eutectic observed with Pt/Pd thermocouples was $1,328.27^{\circ}\text{C}$, with an expanded standard uncertainty of 0.42°C . These results are in accordance with others found in the literature [12–14] for this same type of thermocouple, considering the associated uncertainty.

Table 4 gives the detailed uncertainty budget for the determination of the melting temperature of the Ni–C eutectic cell by the thermocouples. The largest uncertainty contributions, corresponding to more than 85% of the combined uncertainty, come from the calibration of the thermocouples at the conventional fixed points and the extrapolation of the deviation function to the Ni–C eutectic point. Other components related to the plateau identification, the uncertainty of the reference function at the Ni–C point, and the stability of the thermocouples at the conventional fixed points were also considered. A more detailed uncertainty analysis of the measurements performed with Pt/Pd thermocouples at the Ni–C point can be found in [13].

A small temperature difference of 0.12°C was observed when the phase-transition temperature of Ni–C was measured with different thermocouples. This behavior can be explained partially by the different calibration coefficients of the thermocouples, an influence that was taken into account in the uncertainty budget.

Table 4 Uncertainty evaluation of the melting temperature of Ni–C using Pt/Pd thermocouples

Quantity X_i	Estimate i	Standard uncertainty $u(x_i)$	Probability distribution	Sensitivity coefficient c_i	Uncertainty contribution $u_i(y)$ (°C)
T (emf)	1328.27°C	0.02°C	Normal	1	0.02
δCCP	0°C	0.15°C	Normal	1	0.15
δExt	0°C	0.10°C	Normal	1	0.10
δRef	0°C	0.08°C	Normal	1	0.08
<i>Plateau determination</i>					
δE_{RP}	0 μV	0.55 μV	Normal	0.0422 °C · μV^{-1}	0.023
δE_{PI}	0 μV	0.50 μV	Rectangular	0.0422 °C · μV^{-1}	0.021
δE_{HF}	0 μV	0.40 μV	Rectangular	0.0422 °C · μV^{-1}	0.017
δE_{el}	0 μV	0.30 μV	Normal	0.0422 °C · μV^{-1}	0.013
δ_{t0}	0°C	0.005°C	Rectangular	−0.226	−0.001
δE_{H}	0 μV	1.32 μV	Rectangular	0.0422 °C · μV^{-1}	0.056
$\delta E_{\text{S-Cu/Ag}}$	0 μV	0.95 μV	Rectangular	0.0422 °C · μV^{-1}	0.040
Combined uncertainty				0.21	
Expanded uncertainty ($k = 2$)				0.42	

$T(\text{emf})$: Temperature value from calibration curve by extrapolation–repeatability; δCCP : Uncertainty in the calibration function at conventional points; δExt : Uncertainty due to the extrapolation of calibration functions to the Ni–C point; δRef : Uncertainty of the Pt/Pd reference function at the Ni–C point

Plateau determination: Determination of the emf at the melting point; δE_{RP} : repeatability of the emf measurements; δE_{PI} : selection of part of the freezing plateau (inflection point); δE_{HF} : heat flux effects along the thermocouples; δE_{el} : uncertainty of electrical measurements; δ_{t0} : uncertainty in the reference temperature t_0 ; δE_{H} : thermoelectric inhomogeneity (the largest between the two thermocouples); $\delta E_{\text{S-Cu/Ag}}$: stability determined from measurements at the freezing points of Cu or Ag (the largest between the two thermocouples)

3.3 Discussion

The values for the melting point from the two different approaches are in agreement with those of other researchers [3, 10, 12–14]. The difference found in the melting temperature between these two techniques, 0.5°C, is within the combined uncertainty. In the present work, the measurements of the Ni–C cell with the Pt/Pd thermocouples were performed in the horizontal position, while in most other studies the cell was in the vertical position. This difference may be responsible for the lower temperature of the measurement made with the thermocouples, possibly due to different heat transfer conditions. Another possible reason is that the thermocouples wires, while in the horizontal position, may be restricted in their thermal expansion; this “sticking” may be overcome by their weight while in the vertical position. This resistance to free movement may induce stress in the thermocouple wires, affecting the generated emf. This supposition will be tested as soon as this same Ni–C cell is realized in the vertical position and measured by the same Pt/Pd thermocouples.

4 Conclusion

To determine the nickel–carbon eutectic point, the melting and freezing plateaux were realized and measured by a radiation thermometer and by two Pt/Pd thermocouples. The results achieved by these two techniques show a difference similar to that reported by other authors.

Once temperatures are assigned to these secondary reference points, radiation thermometers and thermocouples can be calibrated by interpolation rather than by extrapolation from the silver or copper points, potentially significantly reducing the calibration uncertainty. Considering these encouraging results, Inmetro plans to construct other eutectic cells such as Fe–C, Co–C, and Pd–C.

Acknowledgments The authors would like to thank CNPq/FINEP for the financial support toward the acquisition of the metals used in this work and PTB for the cooperative project with Inmetro.

References

1. H. Preston-Thomas, *Metrologia* **27**(3), 107 (1990)
2. T.J. Quinn, *Metrologia* **34**, 187 (1997)
3. Y. Yamada, H. Sakate, F. Sakuma, A. Ono, *Metrologia* **36**, 207 (1999)
4. E.R. Woolliams, G. Machin, D.H. Lowe, R. Winkler, *Metrologia* **43**, R11 (2006)
5. G. Machin, Y. Yamada, D. Lowe, N. Sasajima, K. Anhalt, J. Hartmann, R. Goebel, H.C. McEvoy, P. Bloembergen, in *Proceedings of TEMPMEKO 2004, 9th International Symposium on Temperature and Thermal Measurements in Industry and Science*, ed. by D. Dvizdic (FSB/LPM, Zagreb, Croatia, 2004), pp. 1049–1056
6. D.P. Dewitt, G.D. Nutter, *Theory and Practice of Radiation Thermometry* (Wiley – Interscience, New York, 1989), Chaps. 10 and 12
7. M.S. Lima, R.N. Teixeira, A.P. Cunha, I.B. Couceiro, in *Proceedings of XVIII IMEKO*, Rio de Janeiro (2006)
8. M. Tischler, *Metrologia* **17**, 49 (1981)
9. S.G. Petkovic, H.D. Vieira, K.N. Quelhas, in *Proceedings of TEMPMEKO 2007* (to be published in Int. J. Thermophys.)
10. C.W. Park, B.H. Kim, D.H. Lee, S.N. Park, *Metrologia* **42**, L5 (2005)
11. J. Fischer, M. Battuello, M. Sadli, M. Ballico, S.N. Park, P. Saunders, Y. Zundong, B.C. Johnson, E. van der Ham, W. Li, F. Sakuma, G. Machin, N. Fox, S. Ugur, M. Matveyev, Uncertainty Budgets for Realization of ITS-90 by Radiation Thermometry. *CCT document 03/03*, BIPM
12. M. Gotoh, in *Proceedings of TEMPMEKO 2001, 8th International Symposium on Temperature and Thermal Measurements in Industry and Science*, ed. by B. Fellmuth, J. Seidel, G. Scholz (VDE Verlag, Berlin, 2002), pp. 67–72
13. F. Edler, A.C. Baratto, *Metrologia* **43**, 502 (2006)
14. F. Edler, P. Ederer, A.C. Baratto, H.D. Vieira, in *Proceedings of TEMPMEKO 2007* (to be published in Int. J. Thermophys.)